

Supplementary Information

Ultrathin Non-doped Thermally Activated Delayed Fluorescence Emitting layer for Highly Efficient OLEDs

Gyana Prakash Nanda,^a Bahadur Sk,^a Nisha Yadav,^a Suresh Rajamanickam,^a Upasana Deori,^a
Rahul Mahashya,^a Eli Zysman-Colman^{b*} and Pachaiyappan Rajamalli^{a*}

^a. Materials Research Centre, Indian Institute of Science, Bangalore-560012, Karnataka, India.

E-mail: rajamalli@iisc.ac.in

^b. Organic Semiconductor Centre, EaStCHEM School of Chemistry, University of St Andrews, St Andrews, United Kingdom.

E-mail: eli_journals@zysman-colman.com

Contents

	Page
Materials and Methods	S2
Synthesis and Characterizations	S3
OLEDs Device architecture	S6
EL Spectra of device	S7
Lippert-Mataga Plot	S7
DFT Calculations	S9
Current density plot	S10
EM layer film morphology	S10
References	S12
¹H and ¹³C NMR and HRMS spectra	S13

Materials and Methods

Instrumentation

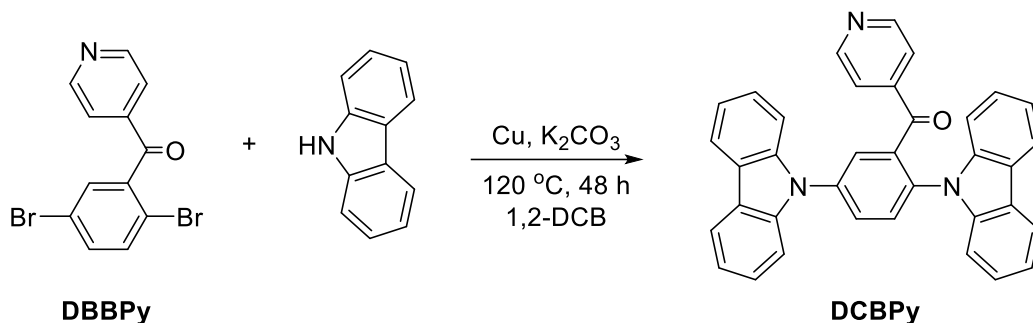
The ^1H and ^{13}C NMR spectra were recorded using Jeol, and Bruker spectrometers. The HRMS were measured using MAT-95XL HRMS. Photoluminescence spectra were recorded on a Hitachi F-7000 spectrophotometer. Transient PL measurement of the materials were obtained using a 355 nm pulsed laser (Nd:YAG laser, INDI-40-10, Spectra-Physics) as the excitation source and the sample was excited by the optical fiber (77532, Newport Corp). A highpass filter (GG-400-25.4, Lambda) at 410 nm placed in front of the photodiode (DET10A/M, Thorlabs) was used to prevent the scattering of 355 nm laser. The electronic signal was recorded using an oscilloscope (WaveSurfer 24MXs-B, LeCroy). The absolute PL quantum efficiencies of the neat films were determined using an integrating sphere under N_2 atmosphere.

OLEDs Fabrication and Measurement

Emitting materials used in device fabrication were usually purified by sublimation. Other materials such as HATCN, NPB, mCP, PPT and TPBi were purchased from the commercial source (Lumtec) and used without further purification. Device were fabricated by vacuum deposition onto precoated ITO glass with sheet resistance of $25\ \Omega/\text{square}$ at a pressure lower than 10^{-6} Torr. Thin emissive layer was evaporated at the rate of $0.1\ \text{\AA}\ \text{s}^{-1}$ and rest of the organic materials were deposited at the rate of $0.5\sim 1.2\ \text{\AA}\ \text{s}^{-1}$. LiF and Al were deposited at the rate of $0.1\ \text{\AA}\ \text{s}^{-1}$, $3\sim 10\ \text{\AA}\ \text{s}^{-1}$, respectively. Rest of the procedures are similar to the reported method.¹

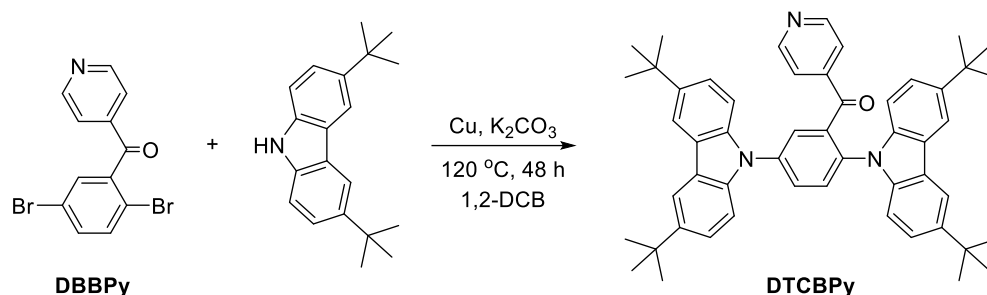
Synthesis Procedures

Synthesis of (2,5-di(9*H*-carbazol-9-yl)phenyl)(pyridin-4-yl)methanone (DCBPy)²



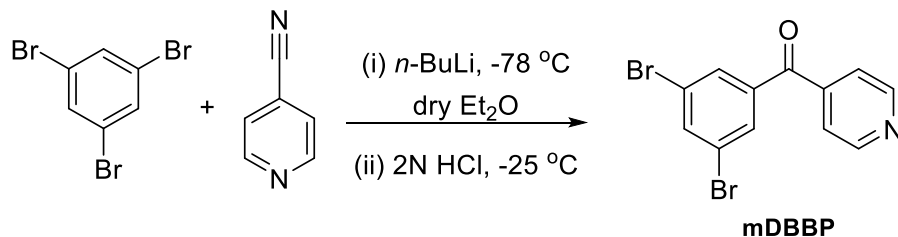
(2,5-dibromophenyl)(pyridine-4-yl)methanone (DBBPy) was synthesized using a reported literature.² To an oven-dried seal tube initially fitted with a septum were added DBBPy (2.5 g, 7.33 mmol), carbazole (3.06 g, 18.33 mmol), Cu (0.93 g, 14.6 mmol), K₂CO₃ (5.06 g, 36.7 mmol) and 1,2-dichlorobenzene (20 mL). The tube was evacuated and purged with nitrogen three times. Then, the septum was removed and the sealed tube was locked with a screw cap under nitrogen atmosphere. The reaction mixture was heated at 180 °C and stirred for 48 h. At the end of the reaction time, the reaction mixture was cooled to room temperature and filtered through a short pad of Celite and washed with ethyl acetate (30 mL). The filtrate was evaporated under reduced pressure and then purified by column chromatography using hexane/ethyl acetate as eluent to afford a yellow solid (DCBPy) (2.15 g, 57% yield); *R*_f = 0.39 (3:7 EtOAc : hexane, silica gel); ¹H NMR (500 MHz, CDCl₃): δ 8.84 (d, *J* = 4.3 Hz, 1H), 8.15 (s, 1H), 8.13 (d, *J* = 5.7 Hz, 2H), 7.72 (d, *J* = 4.4 Hz, 1H), 7.57 – 7.53 (m, 2H), 7.46 (t, *J* = 7.7 Hz, 2H), 7.33 (t, *J* = 7.5 Hz, 2H) ppm; ¹³C NMR (126 MHz, CDCl₃): δ 193.60, 150.81, 143.39, 140.31, 140.20, 139.40, 129.65, 126.66, 126.54, 123.97, 122.80, 121.02, 120.79, 109.45, 109.45 ppm; IR (neat): 3048, 3017, 1670, 1589, 1450, 1333, 1307, 1273, 1226, 922, 837, 745, 716, 646 cm⁻¹; HRMS (ESI-TOF) *m/z*: [M + H]⁺ Calcd for C₃₆H₂₄N₃O 514.1919; Found 514.1916.

Synthesis of (2,5-bis(3,6-di-*tert*-butyl-9*H*-carbazol-9-yl)phenyl)(pyridin-4-yl)methanone (DTCBPy)²



A procedure similar to the synthesis of DCBPy was used for the synthesis of DTCBPy using DBBPy (2.5 g, 7.33 mmol), 3,6-di-*tert*-butyl-9*H*-carbazole (5.1 g, 18.3 mmol), Cu (0.93 g, 14.7 mmol), K₂CO₃ (5.06 g, 36.7 mmol) and 1,2-dichlorobenzene (20 mL) to afford DTCBPy as a light greenish solid (3.4 g, 63% yield); *R*_f = 0.76 (2:8 EtOAc : hexane, silica gel); ¹H NMR (400 MHz, CDCl₃): δ 8.15 (dt, *J* = 2.9, 1.3 Hz, 3H), 8.02 (dd, *J* = 8.4, 2.6 Hz, 1H), 7.88 – 7.81 (m, 3H), 7.77 (d, *J* = 1.9 Hz, 2H), 7.58 – 7.48 (m, 4H), 7.44 (dd, *J* = 8.6, 1.9 Hz, 2H), 7.21 (s, 2H), 6.61 (d, *J* = 6.0 Hz, 2H), 1.46 (s, 18H), 1.40 (s, 18H) ppm; ¹³C NMR (101 MHz, CDCl₃): δ 195.09, 148.80, 144.01, 143.96, 142.19, 139.39, 138.86, 138.41, 136.79, 135.18, 131.11, 130.29, 129.14, 124.14, 124.08, 123.91, 123.48, 120.08, 116.69, 116.46, 109.24, 34.96, 34.89, 32.14, 32.11 ppm; IR (neat): 3067, 3039, 2957, 2899, 2862, 1671, 1496, 1358, 1321, 1290, 1259, 1030, 925, 887, 803, 736, 637, 605 cm⁻¹; HRMS (ESI-TOF) *m/z*: [M + H]⁺ Calcd for C₅₂H₅₆N₃O 738.4423; Found 738.4424.

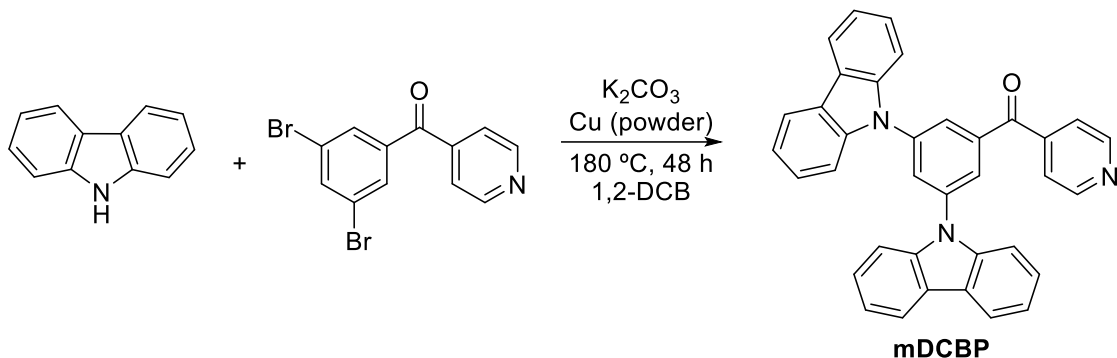
Synthesis of (3,5-dibromophenyl)(pyridin-4-yl)methanone (mDBBP)



In a flame dried two neck flask under nitrogen atmosphere 1,3,5-tribromobenzene (5 g, 15.88 mmol) was dissolved in 160 mL of diethyl ether, and the solution was cooled to –78 °C using acetone and liquid nitrogen composition. A solution of *n*-BuLi (1.6 M in hexane, 11.66 mL, 17.47 mmol) was added slowly so that the temperature did not rise above –76 °C. The reaction mixture

was stirred for 30 min at -78 °C, and a solution of 4-cyanopyridine (1.65 g, 15.88 mmol) in diethyl ether (20 mL) was added slowly. The mixture was stirred at -78 °C for 1 h and slowly allowed to warm to -25 °C, then 2 N HCl (50 mL) was added and the mixture was stirred for 2 h at room temperature. The mixture was made basic by the addition of 1 N NaOH. The product was extracted with EtOAc (2 x 150 ml), and the combined organic layers were dried over Na₂SO₄ filtered, concentrated in *vacuo* and the crude product was purified by a silica gel column *n*-hexane/EtOAc, to afford 77% (4.2 g) of (3,5-dibromophenyl)(pyridin-4-yl)methanone as crystalline white solid (4.2 g, 77% yield); ¹H NMR (400 MHz, CDCl₃): δ 8.80–8.77 (m, 2H), 7.86 (t, *J* = 1.8 Hz, 1H), 7.78 (d, *J* = 1.8 Hz, 2H), 7.51 (d, *J* = 1.7 Hz, 1H), 7.50 (d, *J* = 1.7 Hz, 1H).ppm; ¹³C NMR (101 MHz, CDCl₃): δ 192.03, 150.58, 142.68, 138.73, 138.44, 131.40, 123.35, 122.48 ppm.

Synthesis of (3,5-di(9*H*-carbazol-9-yl)phenyl)(pyridin-4-yl)methanone (mDCBP)



To an oven-dried seal tube initially fitted with a septum were added (3,5-dibromophenyl)(pyridin-4-yl)methanone (mDBBP) (3.0 g, 8.8 mmol), carbazole (3.68 g, 21.9 mmol), Cu (1.12 g, 17.6 mmol), K₂CO₃ (6.08 g, 43.98 mmol) and 1,2-dichlorobenzene (20 mL). The tube was evacuated and purged with nitrogen three times. Then, the septum was removed and the sealed tube was locked with a screw cap under nitrogen atmosphere. The suspension was stirred at 180 °C for 48 h. After completion of the reaction, the reaction mixture was diluted with ethyl acetate (30 mL), filtered through combination of Celite and Silica pad, and washed with ethyl acetate (3 X 30 mL). The combined filtrate was concentrated under reduced pressure and the residue was purified by a silica gel column chromatography using ethyl acetate/*n*-hexane as the eluent to afford (3,5-di(9*H*-carbazol-9-yl)phenyl)(pyridin-4-yl)methanone (mDCBP) as a white solid (2.66 g, 59% yield); *R*_f = 0.41 (3:7 EtOAc : hexane, silica gel); ¹H NMR (500 MHz, CDCl₃): δ 8.86 – 8.81 (m, 2H), 8.15 (t, *J* = 1.0 Hz, 2H), 8.13 (t, *J* = 1.0 Hz, 2H), 8.12 (d, *J* = 1.9 Hz, 1H), 8.11 (d, *J* = 1.9 Hz, 2H), 7.74

– 7.68 (m, 2H), 7.54 (dt, $J = 8.3, 0.9$ Hz, 4H), 7.45 (ddd, $J = 8.3, 7.1, 1.2$ Hz, 4H), 7.32 (ddd, $J = 7.9, 7.2, 1.0$ Hz, 4H) ppm; ^{13}C NMR (126 MHz, CDCl_3): δ 193.63, 150.85, 143.42, 140.33, 140.23, 139.43, 129.68, 126.69, 126.56, 123.99, 122.82, 121.05, 120.81, 109.46 ppm; IR (neat): 3046, 3016, 2922, 2851, 3013, 2923, 2850, 1595, 1330, 1224, 1153, 917, 746, 717, 636, 570 cm^{-1} ; HRMS (ESI-TOF) m/z : $[\text{M} + \text{H}]^+$ Calcd for $\text{C}_{36}\text{H}_{24}\text{N}_3\text{O}$ 514.1919; Found 514.1919.

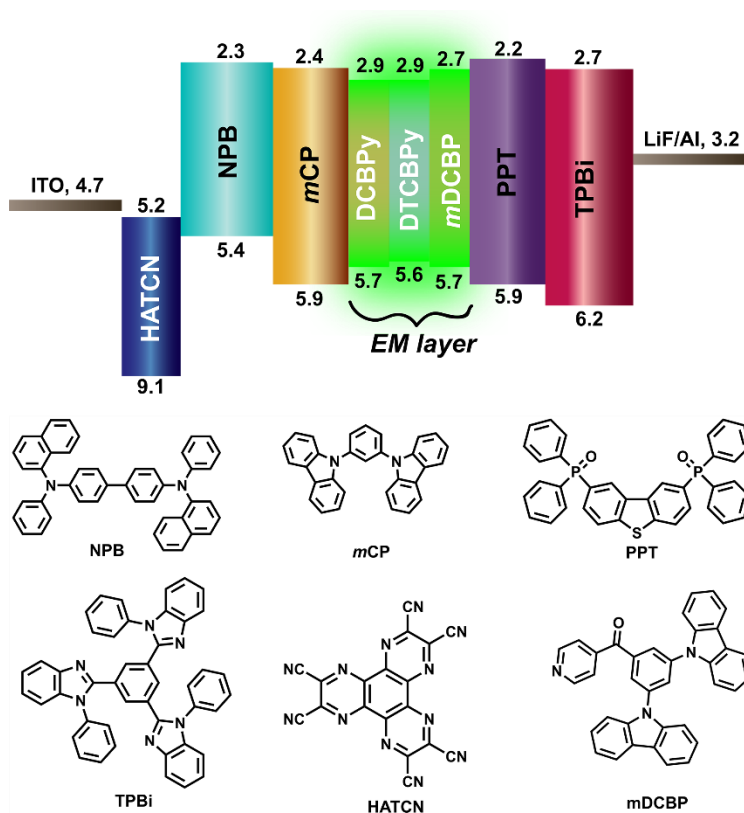


Fig. S1 OLED device architecture and molecular structures of the materials used in devices.

Table S1. The EL performances of the devices A-C.

Device	EML thickness (nm)	L (cd/m ²)	EQE _{max} (%)	CE (cd/A)	PE (lm/W)	λ_{EL} (nm)	CIE (x,y), 8V
A	30	12,509	5.2	16.7	7.5	518	(0.27,0.55)
A1	1	17,250	13.5	45.2	21.9	520	(0.27,0.57)
B	1	11,350	9.7	23.5	18.2	496	(0.17,0.39)
C	1	6393	5.9	15.5	11.0	503	(0.21,0.44)

L, maximum luminance; EQE_{max}, maximum external quantum efficiency; CE, maximum current efficiency; PE, maximum power efficiency; and λ_{EL} , the wavelength where the EL spectrum has the highest intensity.

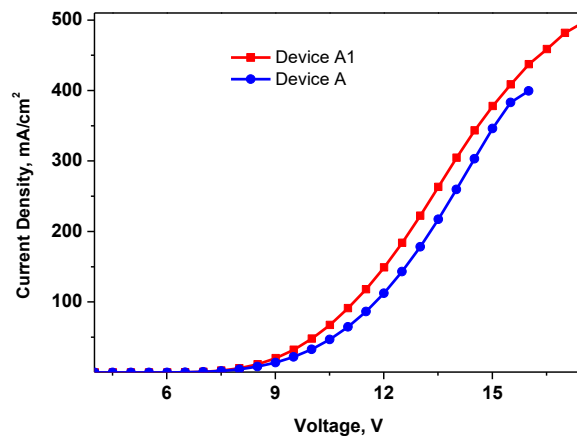


Fig. S2 Current density vs voltage of devices A and A1.

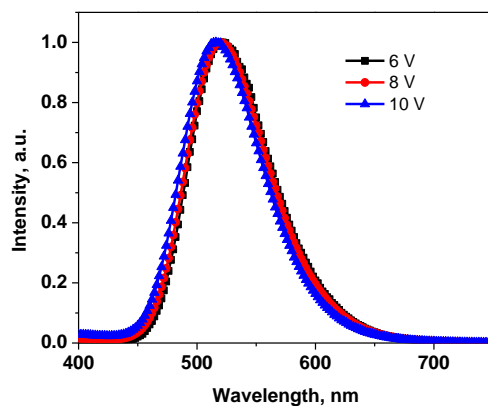


Fig. S3 EL spectra of device A1 measured at different voltages.

Intramolecular charge transfer (ICT) analysis: Lippert-Mataga Plot

A comparative intramolecular charge transfer (ICT) property of mDCBP, and DTCBPy was analyzed using the Lippert-Mataga plot (L-M plot, solvatochromism).³ Both the compounds are exhibiting positive solvatochromic behaviors in different polar solvents. The significant solvatochromic Stokes shift in all the different polar solvents was observed for all the compounds. However, the fitting of L-M plot resulted in a very high slope for mDCBP (9848 cm⁻¹) and a small slope for DTCBPy (3746 cm⁻¹). This is indicating the prominent CT interactions in mDCBP and

comparatively weak CT interactions in DTCBPy. The solvatochromic emission and the Lipper-Mataga plot are shown in Fig. S4-S5, Table S2-S3.

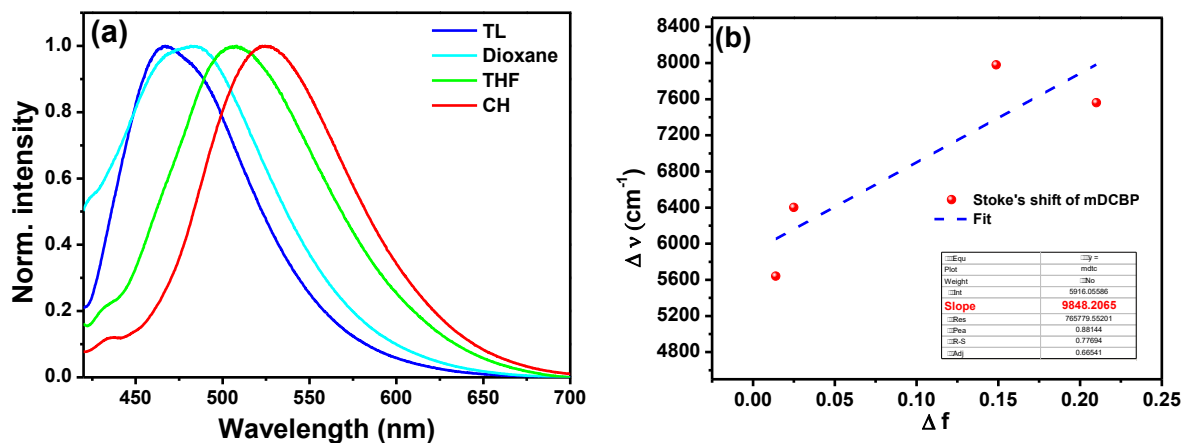


Fig. S4 (a) Normalized emission spectra and (b) L-M plot of mDCBP in different polar solvents at room temperature.

Table S2. Spectroscopic data table of mDCBP in various polar solvents.

Solvent	λ_{abs}	λ_{em}	Stokes shift in nm	$\Delta\nu$ (cm ⁻¹)	Δf
TL	369	466	97	5641.04	0.014
Dioxane	366	478	112	6401.9	0.025
THF	366	506	140	7559.5	0.210
CH	370	525	155	7979.40	0.1488

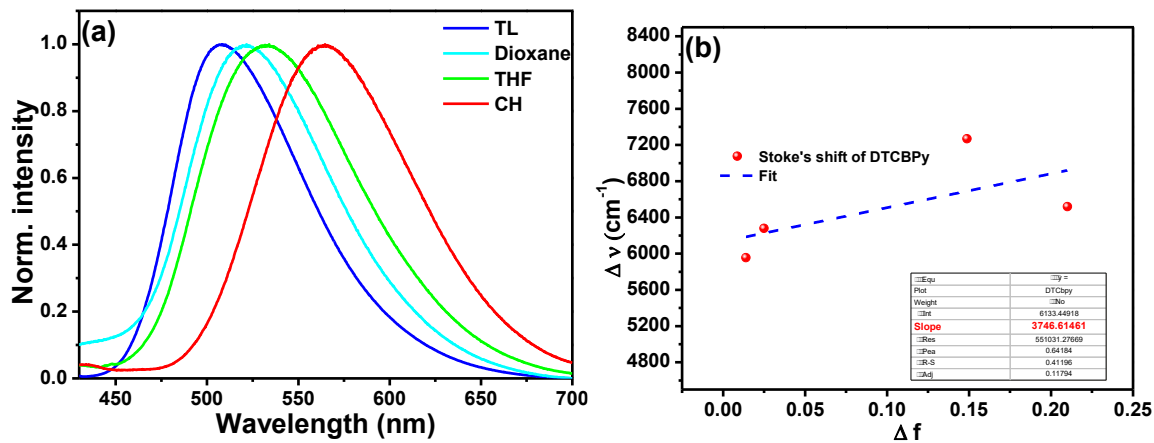


Fig. S5 (a) Normalized emission spectra and (b) L-M plot of DTCBPy in different polar solvents at room temperature.

Table S3. Spectroscopic data table of DTCBPy in various polar solvents.

Solvent	λ_{abs}	λ_{em}	Stokes shift in nm	$\Delta\nu$ (cm ⁻¹)	Δf
TL	390	508	118	5955.9	0.014

Dioxane	392	520	128	6279.4	0.025
THF	395	532	137	6519.4	0.210
CH	400	564	164	7269.5	0.1488

DFT Calculations

A time-dependent density functional theory (TDDFT) investigation for DTCBPy and mDCBP were performed using the Gaussian 09 program package in the delta-cluster of SERC facility @IISc. The single crystal structure was used as the input geometries for time dependent density functional theory (TDDFT) calculations. The TDDFT calculations was carried out with CAM-B3LYP hybrid functional and 6-311G(d,p) basis set in Gaussian 09 software.⁴⁻⁶ GaussView 5.0 and Chemcraft (version 1.8) were used to analyze the molecular orbitals. The iso values ± 0.0004 was used hole-electron distributions. The hole-electron distributions are shown Fig. S6. The singlet and triplet excited states including hole and electron distributions were analysed using *Multiwfn* program package (Fig. S6).⁷

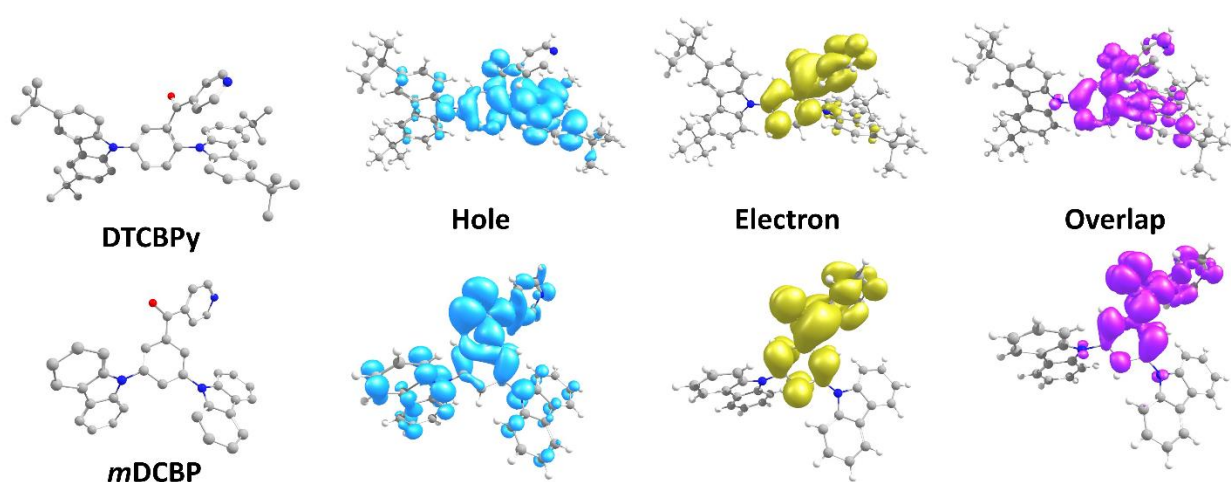


Fig. S6 The TDDFT calculated hole-electron distributions describing the excitation characters of the S_1 states of (a) DTCBPy and (b) mDCBP are shown. The weights of the hole–electron overlap to the excitations are included with iso value = 0.0004.

Table S4. The energy levels and singlet-triplet energy gap of DCBPy, DTCBPy and mDCBP.

Compound	Eg (eV)	HOMO (eV)	LUMO (eV)	S_1 (eV)	T_1 (eV)	^a ΔE_{ST} / ^b ΔE_{ST} (eV)
DCBPy	2.87	-5.75	-2.88	2.87	2.84	0.03/ 0.11
DTCBPy	2.74	-5.61	-2.87	2.74	2.70	0.04 / 0.10
mDCBP	3.00	-5.72	-2.72	3.00	2.94	0.06/0.15
^a Experimental, ^b Theoretical						

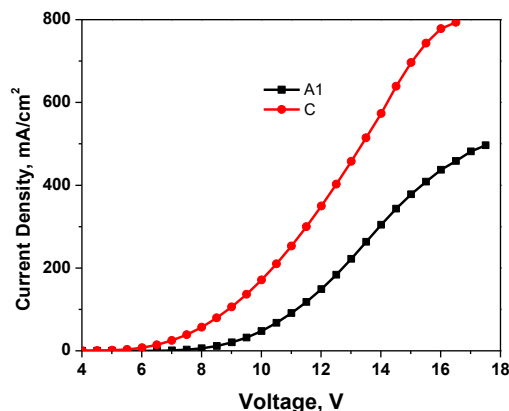


Fig. S7 Current density of the devices A1 and C.

EM layer film morphology

The emissive (EM) layer was fabricated by vacuum deposition on a silicon wafer and glass substrate. The ~ 1 nm EML was fabricated on a bare substrate and on organic material (30 nm DPEPO) precoated substrate to make a smooth surface for thin EML. We have chosen DPEPO due to the high energy gap, which will not give emission in the visible region upon laser excitation; therefore, we can see clear-cut emission from EML. The films were then characterized using atomic force microscopy (AFM) and confocal laser scanning microscopy (CLSM) for the thickness, morphology, and uniformity of EML on the surface (Fig. S8-S10). We tried to measure the thickness of the ~ 1 nm film on a bare substrate by AFM, but it was not accurate, as depicted in Fig. S9 due to substrate surface roughness. However, The 31 nm films on a silicon wafer and glass substrate resemble the thickness about ~ 32 -35 nm (average) for both the substrate and the surface morphology is quite uniform as depicted in the AFM and CLSM images (Fig. S8 and S10). In order to check the homogeneity of emitter coverage on the surface, we have taken CLSM images. The CLSM image shows the intense green emission on the surface of all films, which suggests that the emitter is homogeneously coated on the substrate as well as on organic film (1 nm film shows uniformity only on the part of the substrate because the imaging was carried out on the edge of the film). This result confirms the uniformity of the emitting layer of the film and is consistent with the electroluminescence photograph.

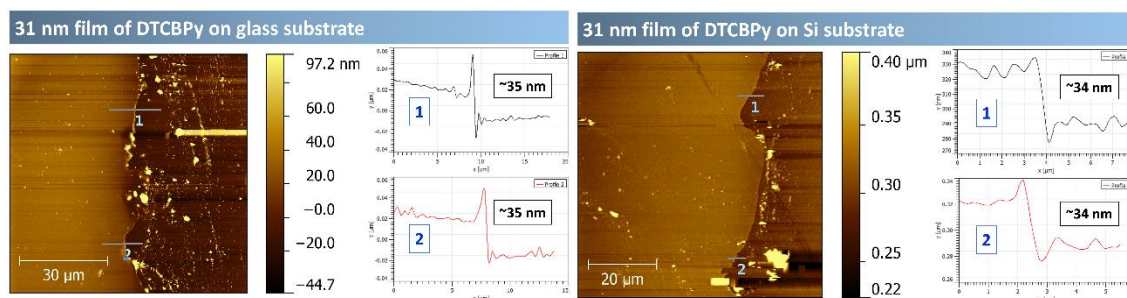


Fig. S8 Top view atomic force microscopy (AFM) images of 31 nm (DPEPO (30 nm) + DTCBPY (1 nm)), film on (a) glass substrate, and (b) silicon wafer fabricated by vacuum deposition. The thickness of the films was analysed and are shown.

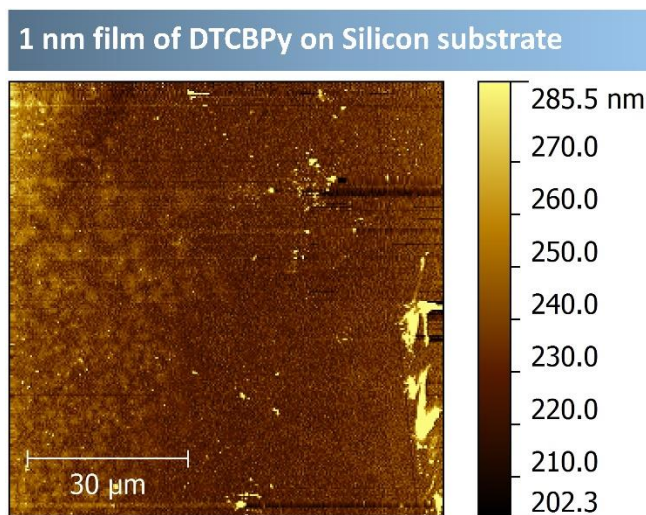


Fig. S9 Top view atomic force microscopy (AFM) images of ~1 nm film on silicon wafer fabricated by vacuum deposition. The thickness of the film was analyzed and shown.

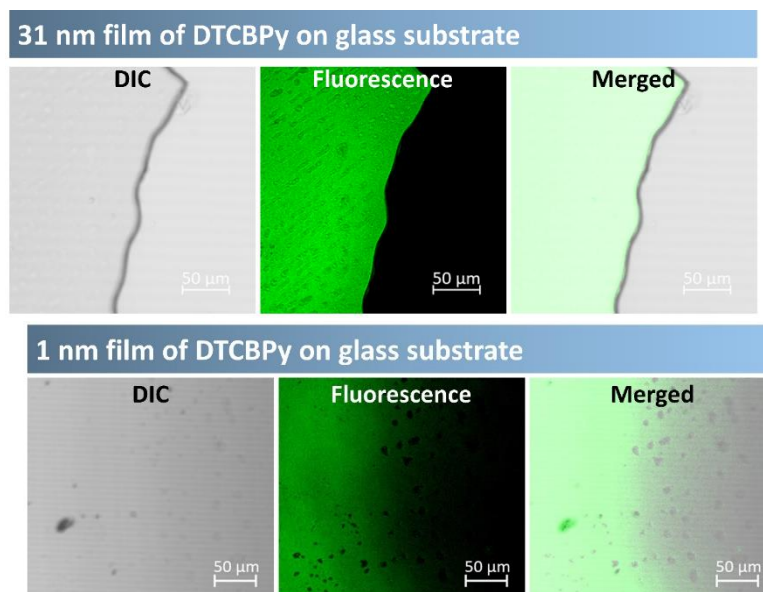


Fig. S10 Confocal laser scanning microscopy (CLSM) images of (a) 31 nm ((DPEPO (30 nm) + DTCPy (1 nm)), and (b) 1 nm film on glass substrate fabricated by vacuum deposition. The CLSM images depict the uniformity of the EM layer. Laser excitation $\lambda_{\text{ex}} = 408 \text{ nm}$, $\lambda_{\text{em}} = 420\text{-}550 \text{ nm}$ (green channel).

Reference:

1. J.-J. Lin, W.-S. Liao, H.-J. Huang, F.-I. Wu and C.-H. Cheng, *Adv. Funct. Mater.*, 2008, **18**, 485-491.
2. P. Rajamalli, N. Senthilkumar, P. Gandeepan, P.-Y. Huang, M.-J. Huang, C.-Z. Ren-Wu, C.-Y. Yang, M.-J. Chiu, L.-K. Chu, H.-W. Lin and C.-H. Cheng, *J. Am. Chem. Soc.*, 2016, **138**, 628-634.
3. J. R. Lakowicz, *Principles of fluorescence spectroscopy*, Springer, New York, 2006.
4. C. Lee, W. Yang and R. G. Parr, *Phys. Rev. B*, 1988, **37**, 785-789.
5. B. Miehlisch, A. Savin, H. Stoll and H. Preuss, *Chem. Phys. Letter.*, 1989, **157**, 200-206.
6. A. D. Becke, *J. Chem. Phys.*, 1993, **98**, 5648-5652.
7. T. Lu and F. Chen, *J. Comp. Chem.*, 2012, **33**, 580-592.

¹H and ¹³C NMR and Mass spectra

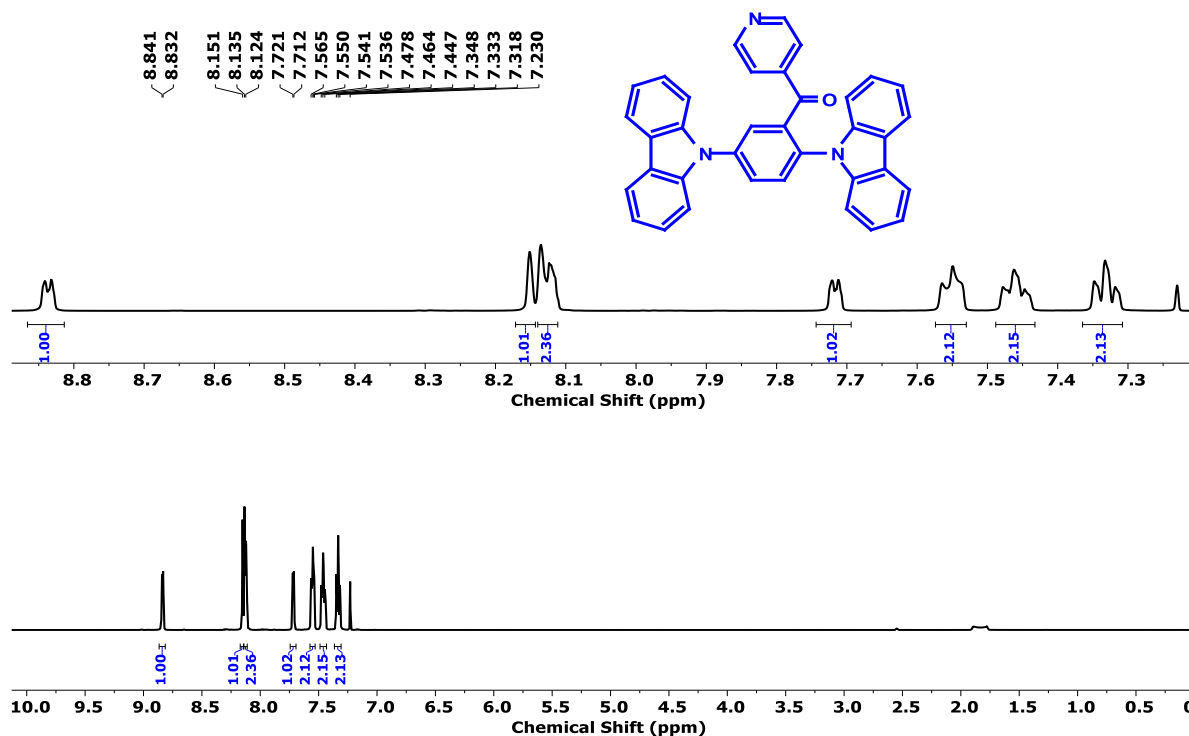


Fig. S8 ¹H NMR (500 MHz, CDCl₃) spectra of (2,5-di(9*H*-carbazol-9-yl)phenyl)(pyridin-4-yl)methanone (DCBPy).

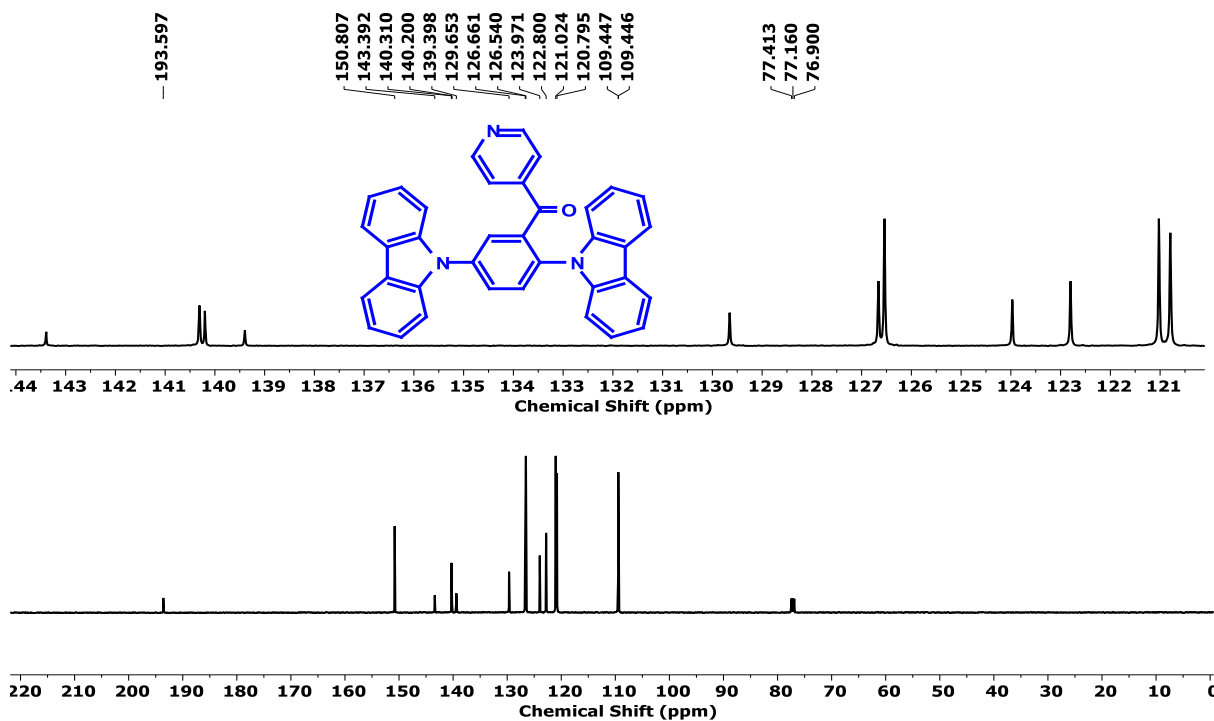


Fig. S9 ¹³C NMR (126 MHz, CDCl₃) spectra of (2,5-di(9*H*-carbazol-9-yl)phenyl)(pyridin-4-yl)methanone (DCBPy).

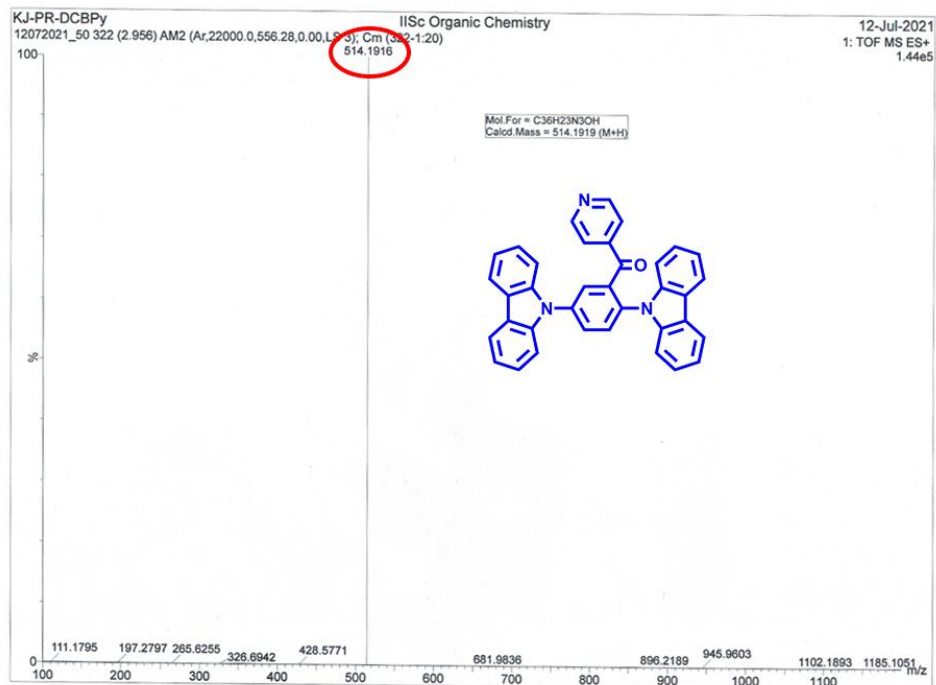


Fig. S10 HRMS (TOF MS ESI+) spectra of (2,5-di(9*H*-carbazol-9-yl)phenyl)(pyridin-4-yl)methanone (DCBPY).

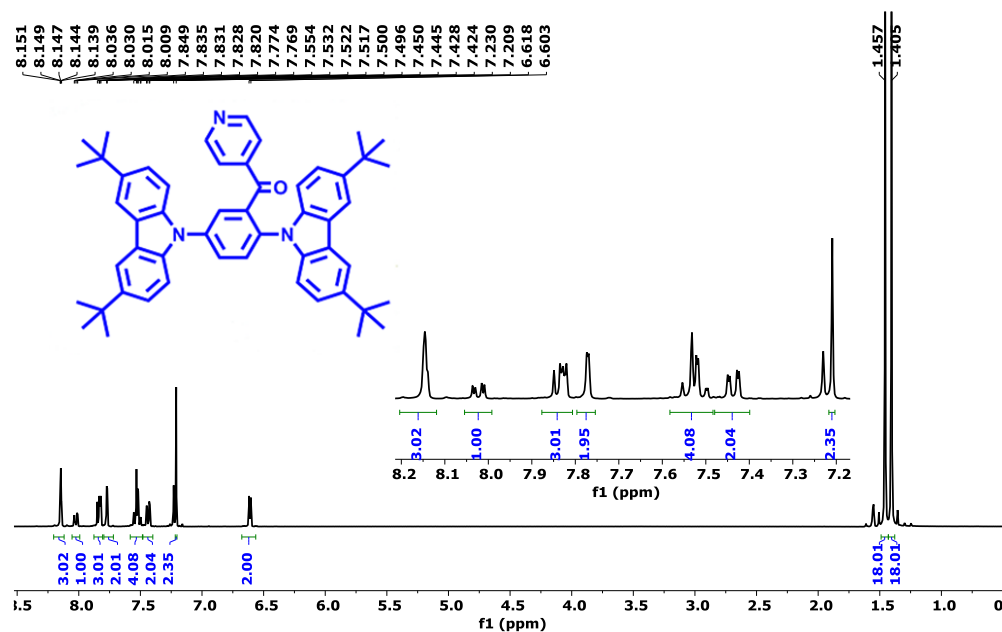


Fig. S11 ^1H NMR (400 MHz, CDCl_3) spectra of (2,5-bis(3,6-di-*tert*-butyl-9*H*-carbazol-9-yl)phenyl)(pyridin-4-yl)methanone (DTCBPY).

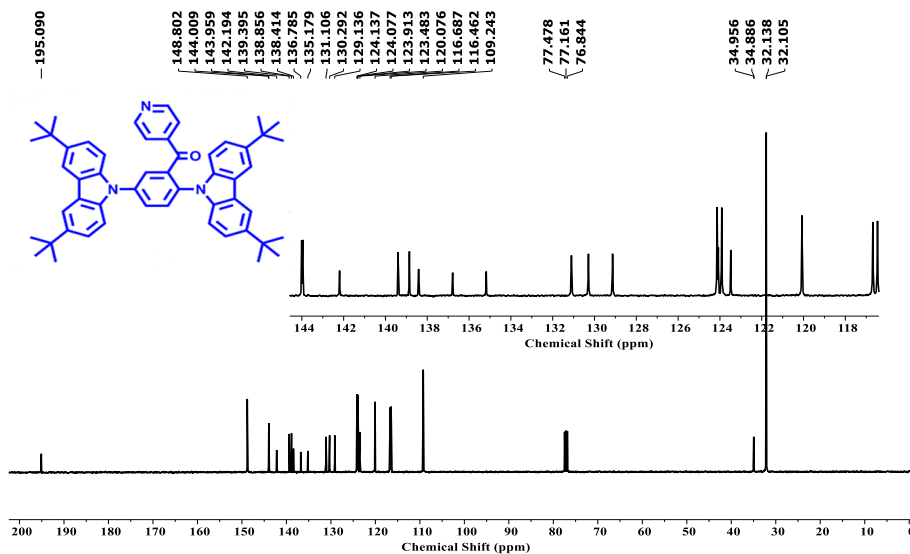


Fig. S12 ^{13}C NMR (101 MHz, CDCl_3) spectra of (2,5-bis(3,6-di-*tert*-butyl-9H-carbazol-9-yl)phenyl)(pyridin-4-yl)methanone (DTCBPy).

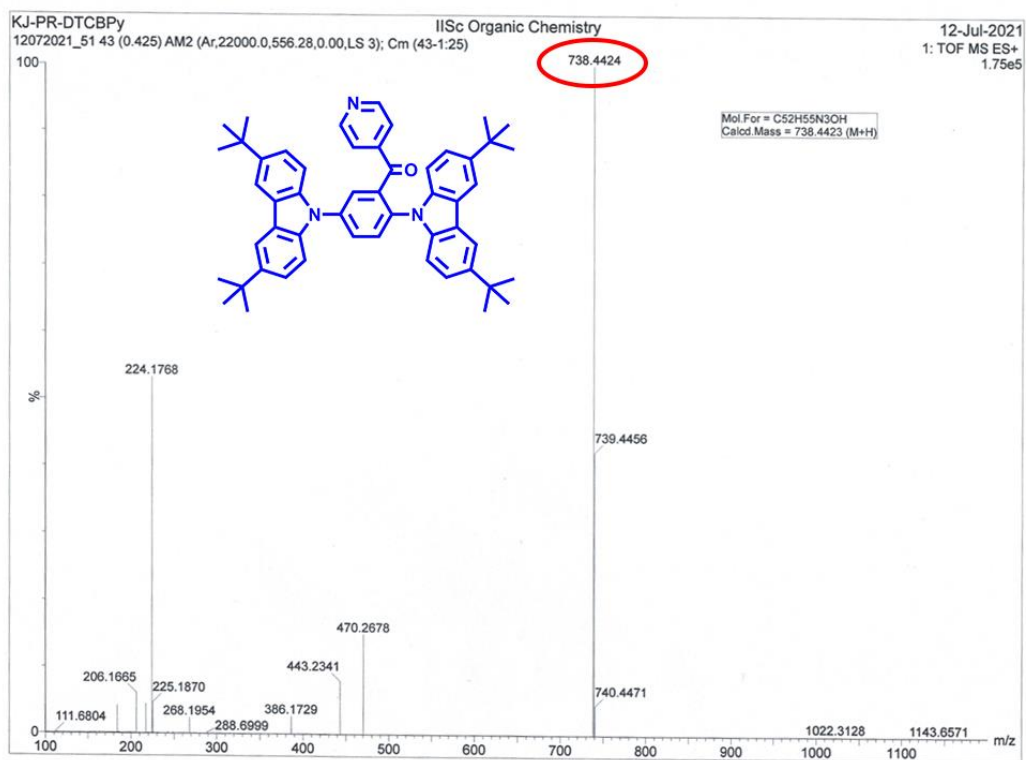


Fig. S13 HRMS (TOF MS ESI+) spectra of (2,5-bis(3,6-di-*tert*-butyl-9H-carbazol-9-yl)phenyl)(pyridin-4-yl)methanone (DTCBPy).

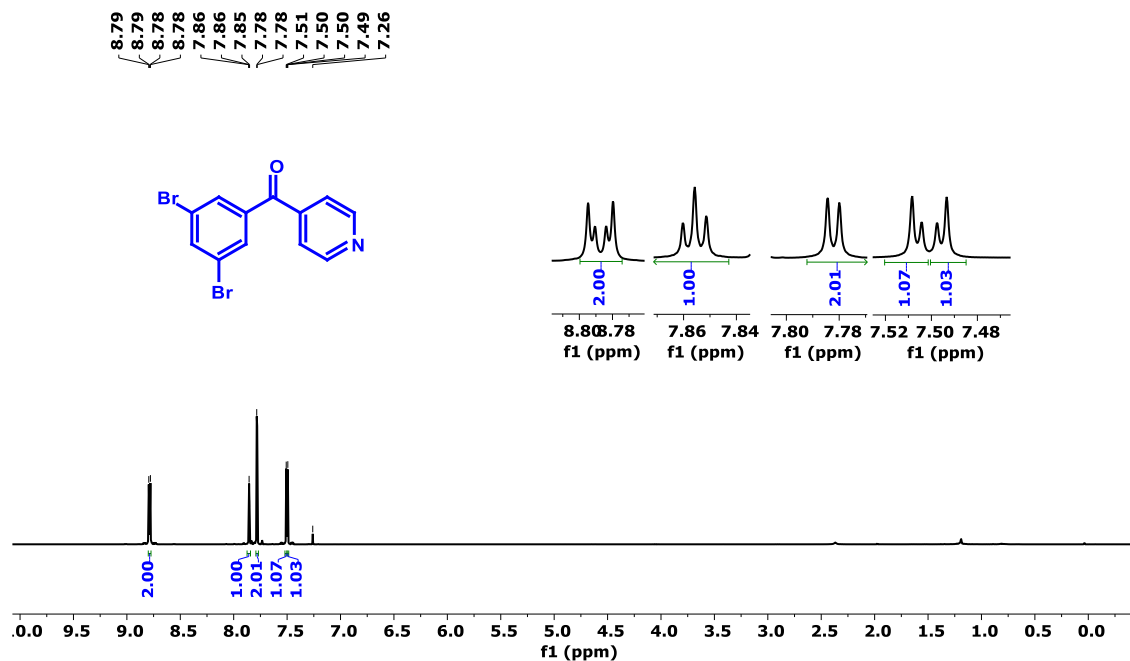


Fig. S14 ¹H NMR (400 MHz, CDCl₃) spectra of (3,5-Dibromophenyl)(pyridin-4-yl)methanone (*m*DBBP).

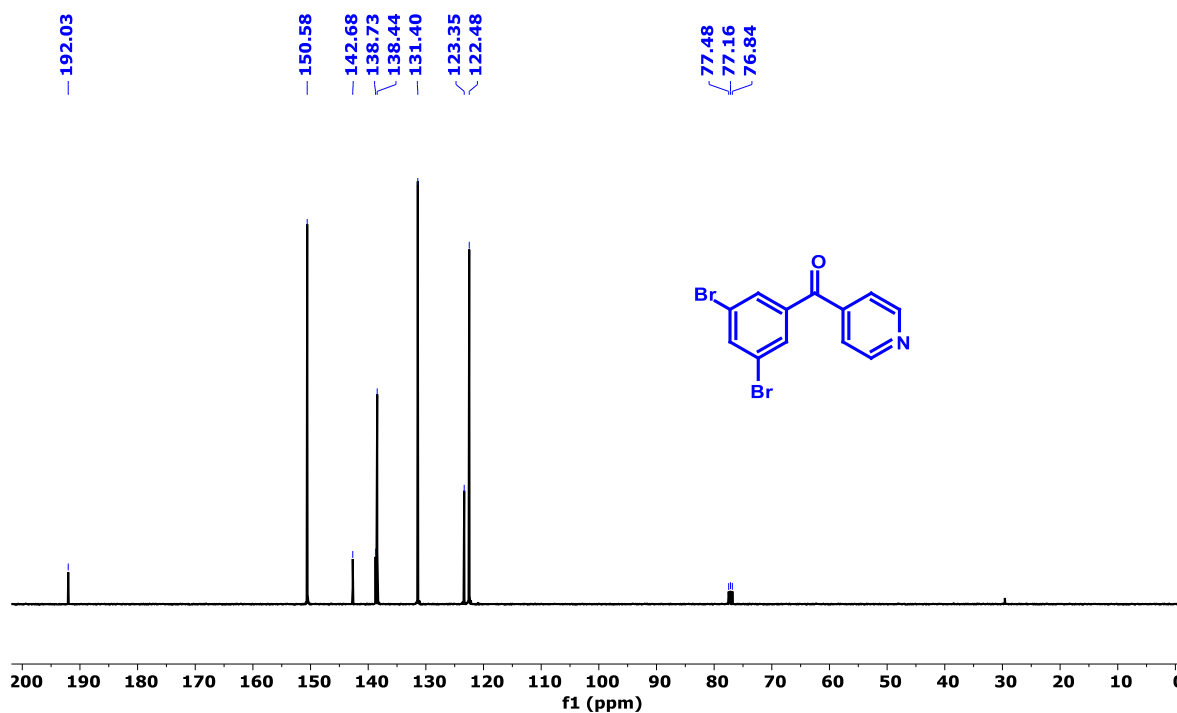


Fig. S15 ¹³C NMR (101 MHz, CDCl₃) spectra of (3,5-dibromophenyl)(pyridin-4-yl)methanone (*m*DBBP).

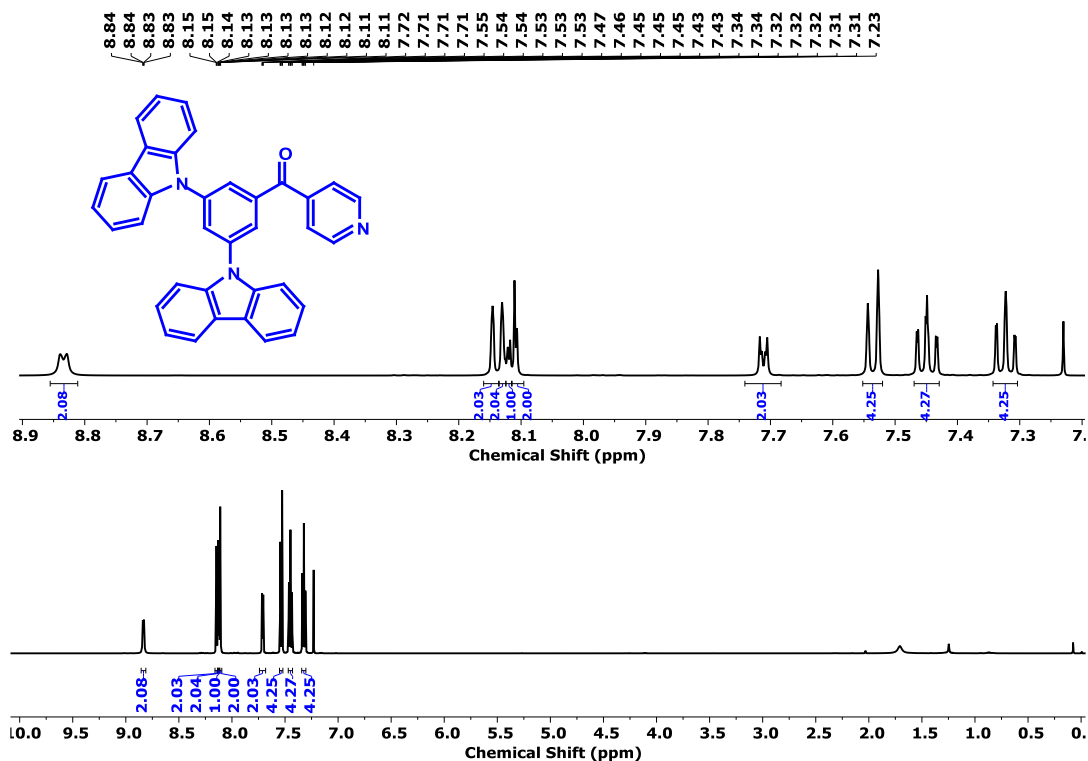


Fig. S16 ¹H NMR (500 MHz, CDCl₃) spectra of (3,5-di(9*H*-carbazol-9-yl)phenyl)(pyridin-4-yl)methanone (mDCBP).

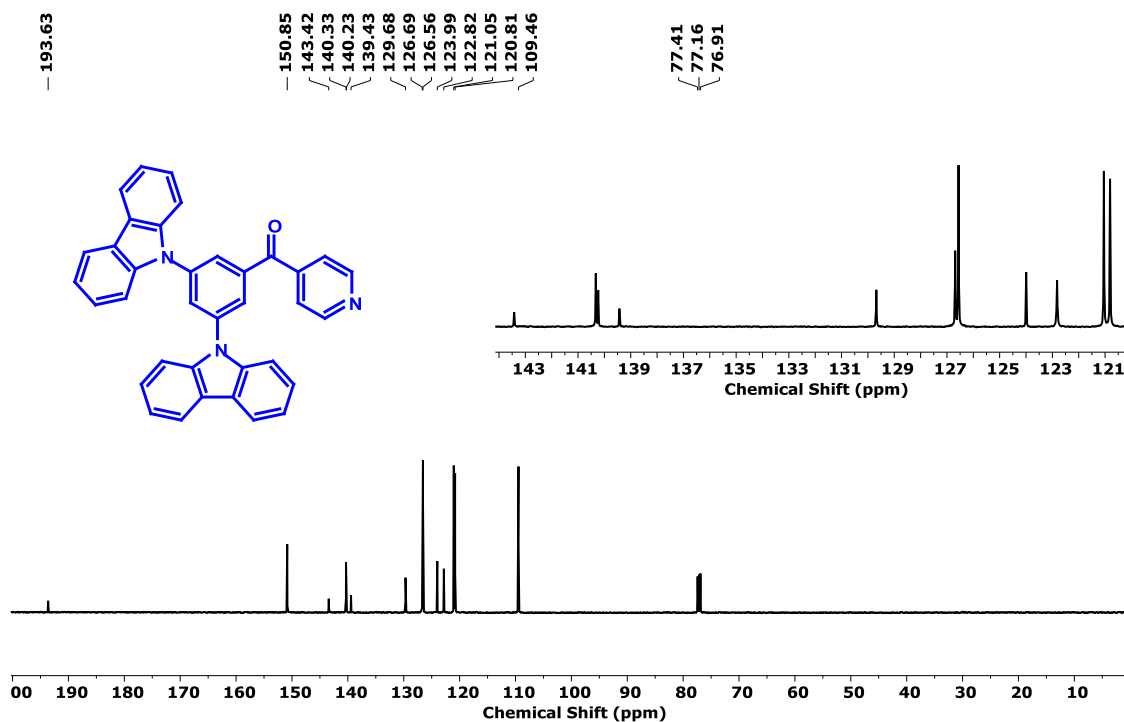


Fig. S17 ¹³C NMR spectra of (3,5-di(9*H*-carbazol-9-yl)phenyl)(pyridin-4-yl)methanone (mDCBP): (126 MHz, CDCl₃).

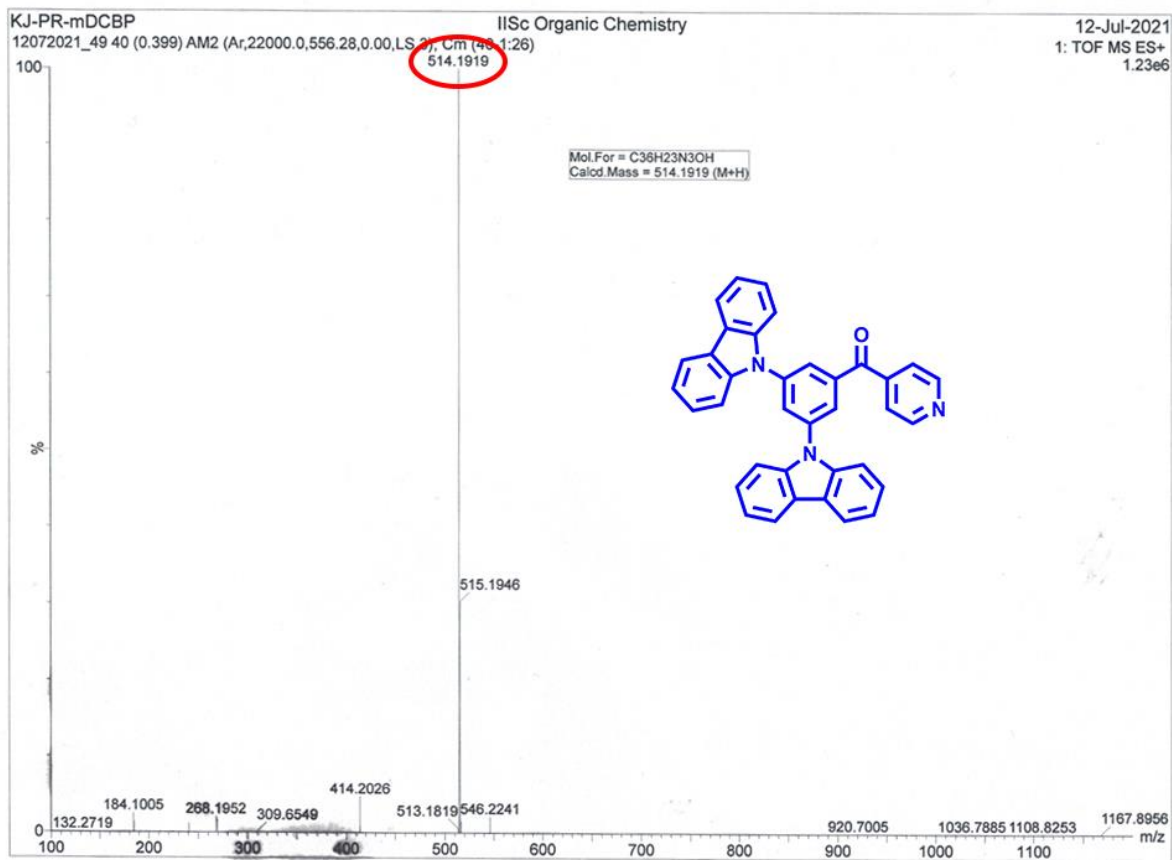


Fig. S18 HRMS (TOF MS ESI+) spectra of (3,5-di(9H-carbazol-9-yl)phenyl)(pyridin-4-yl)methanone (mDCBP).